Available online at www.sciencedirect.com

ScienceDirect

IFAC Papers Online CONFERENCE PAPER ARCHIVE

IFAC-PapersOnLine 48-1 (2015) 390–393

# Numerics of contact line motion for thin films

**Dirk Peschka** *

* *Weierstrass Insitute, Mohrenstr. 39, 10117 Berlin, Germany (e-mail: dirk.peschka@wias-berlin.de)*

**Abstract:** We introduce an algorithm for the explicit treatment of contact line motion for thin-film problems and compare its solutions with exact source-type solutions and their asymptotic behavior near the contact line. The algorithm uses a variational formulation and avoids dealing with singularities near the contact line.



*Keywords:* thin fluid films, free boundary problems, numerical algorithms, self-similar solutions

## 1. MODEL AND ALGORITHM

The spreading of a viscous liquid droplet of height $h(t,x)$ over a solid substrate by surface tension is governed by a partial differential equation of the type

$$\dot h + (|h|^n h_{xxx})_x = 0, \tag{1a}$$
$$h(0,x) = h_0(x), \tag{1b}$$

where we use the notation $\dot h = h_t$ for time derivatives. For illustration of the geometry see fig. 1. The mobility exponent $n$ depends on the type of friction with the substrate, where usually one has $0 < n \leq 3$ as it is discussed by Eggers (2004). Additionally we assume that the initial support is an interval $(x_-, x_+) := \operatorname{supp} h_0$, where $x_\pm$ evolve with time. As boundary conditions we consider a zero contact angle and specify a kinematic condition, so that for $t > 0$

$$h_x(t, x_\pm) = 0, \tag{1c}$$
$$\dot x_\pm = \lim_{x\to x_\pm} \left(|h|^{n-1} h_{xxx}\right). \tag{1d}$$

Solutions of (1) conserve the volume $v(t) = \int h\,\mathrm{d}x \equiv v(0)$ and it is known that the support moves with finite speed, see Hulshof et al. (1998). For $n > 1$ the kinematic condition (1d) implies $h_{xxx} \to \infty$ as $x \to x_\pm$ for the contact line to move with a finite velocity. This singularity with the fact that $h \to 0$ as $x \to x_\pm$ is one major difficulty in using (1d) to evaluate the velocity of the boundary.

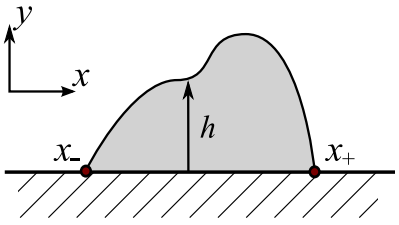


Fig. 1. droplet parametrized by $h$ on a solid substate

The thin-film problem is known already for quite some time, i.e. existence of weak solutions was shown by Bernis and Friedman (1990). In the context the free-boundary problem above existence of solutions in weighted Hölder spaces was shown by Giacomelli and Knüpfer (2010). In general one can not guarantee that after starting with an interval $(x_-, x_+)$ the solution will always stay strictly positive inside $(x_-(t), x_+(t))$ and no topological transitions occur.

Numerical algorithms for this problem mainly rely on global solutions for this problem, i.e. algorithms which solve for $h(t,x)$ for $x \in \mathbb{R}$ and preserve non-negativity outside $(x_-, x_+)$ in a sense, see e.g. the works by Zhornitskaya and Bertozzi (1999); Grün and Rumpf (2000). Here we go a different route and do *not* look for global solutions but rather seek solutions of the free-boundary problem (1). Such an approach is certainly not feasible to treat topological transitions. Our proposed method is to first solve (1a) using the space and time-discrete variational formulation using finite elements just on the support $(x_-, x_+)$. Here we seek piecewise linear functions $\dot h, \pi$ that satisfy

$$\int_{x_-}^{x_+} (\,\dot h\phi + |h|^n \pi_x \phi_x)\,\mathrm{d}x = 0, \tag{2a}$$
$$\int_{x_-}^{x_+} (\,\pi\varphi - \tau \dot h_x \varphi_x)\,\mathrm{d}x = \int_{x_-}^{x_+} h_x \varphi_x\,\mathrm{d}x, \tag{2b}$$

for all piecewise linear test functions $\phi, \varphi$ defined on an decomposition of the interval $(x_-, x_+)$. No essential boundary conditions are imposed on solutions or test functions. Note that all appearances of $h$ and $x_\pm$ are treated explicitly. In order to arrive at (2) we introduced a new variable $\pi = -h_{xx}$ and split (1a) in two second order equations. Furthermore we used (1c) the zero contact angle $h_x = 0$ and a no-flux condition $|h|^n h_{xxx} = 0$ at $x_\pm$ as natural boundary conditions. Only in (2b) defining $\pi$ we replaced $h$ by the more implicit expression $h + \tau\dot h$ where $\tau = t^{k+1} - t^k$ to obtain a stable method similar to a (semi)-implicit Euler method. For any given $h$ defined on $(x_-, x_+)$ this gives us the time-derivative $\dot h$ in the Eulerian reference frame.

However, we need another method to compute $x_\pm$ and $h$ at time $t^{k+1}$ from the corresponding data at time $t^k$. Here we use the fact that in a reference frame moving

⋆ Financial support by DFG in the MATHEON project C10 and by Einstein Center for Mathematics in Berlin ECMath in project OT1


10.1016/j.ifacol.2015.05.052

with velocity $\dot\psi$ time derivatives of $H(t,y) = h(t,\psi(t,y))$ simply transform according to

$$\dot H = \dot h + \dot\psi h_x, \tag{3}$$

where $y \in (x_-(t^k), x_+(t^k))$. If we choose $\psi(t, x_\pm(t^k)) = x_\pm(t)$ then $H(t, x_\pm(t^k)) \equiv 0$ which implies $\dot h = -\dot\psi h_x$ at $x_\pm$. In one spatial dimension we can simply choose

$$\psi(t,y) = x_-(t) + y\big(x_+(t) - x_-(t)\big), \tag{4}$$

with $y = (x - x_-(t^k))/(x_+(t^k) - x_-(t^k))$ as such a mapping. Now we can explicitly and uniquely determine $\dot H, \dot\psi$ from $\dot h$ using the known $h_x$ and (3). For small time steps $\tau \ll 1$ we can assume $h_x \approx h_y$.

Note that for a finite contact angle this procedure makes sense in the discrete and continuous setting. However, one might wonder if evaluating (3) for $\dot\psi$ at a zero contact angle is well-defined at the boundary. At least for linear elements the weak derivative $h_x$ is piecewise constant, so that provided $h$ is positive inside $(x_-, x_+)$ at $t^k$, then $h_x$ has a proper nonzero sign.

*Algorithm summarized*

Thereby the strategy to solve the free boundary problem(1) is as follows.

For given solution $h, x_\pm$ at time $t^k$

(i) Solve the semi-implicit in time finite element variational formulation (2) for $\dot h, \pi$.

(ii) Use the prior information of $h_x$ at $t^k$ to compute $\dot H$ and $\dot\psi$ from the previously computed $\dot h$ as explained above.

(iii) Evolve $h$ and the domain $(x_-, x_+)$ by updating all vertices of the finite element decomposition and all nodal values according to

$$x^{k+1} = x^k + \tau\dot\psi(x^k),$$
$$h^{k+1} = h^k + \tau\dot H,$$

as it is natural in a comoving coordinate system. Writing this slightly more detailed, what we mean is

$$h_i^{k+1} \equiv h^{k+1}(x_i^{k+1}) = h^k(x_i^k) + \tau\dot H_i \equiv h_i^k + \tau\dot H_i,$$
$$x_i^{k+1} = x_i^k + \tau\dot\psi(x_i^k),$$

for all nodes $i$ of the domain decomposition. Note that the definition of $\psi$ ensures $x^{k+1}$ is again an admissible decomposition provided that $x_- < x_+$.

This concludes a single time-step of the algorithm. Note that this algorithm can be naturally extended to higher dimensions as we discuss later. Note that if we include boundary terms in the definition of $\pi$ in (2b), then we can also include nonzero contact angles $|h_x| = \tan\theta$ in the problem. Using a variational approach to solve (1) is thereby superior to other numerical methods, e.g. finite differences, in the sense that it allows a simple implementation of all boundary conditions as natural boundary conditions. Furthermore note that (1) has a gradient structure with an energy $E$ that decreases according to

$$\frac{d}{dt}E(h) = -\int |h|^n(\pi_x)^2 \mathrm{d}x < 0,$$

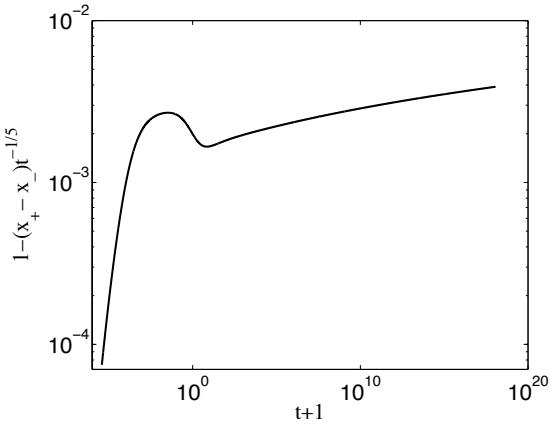


Fig. 2. Relative error of support width of numerical solution compared to exact solution at various times.

and $\pi = \delta E/\delta h$. For the problem here we have

$$E(h) = \int_{-\infty}^{\infty} \frac{1}{2}|h_x|^2 \,\mathrm{d}x.$$

## 2. NUMERICS FOR SOURCE-TYPE SOLUTIONS

The following section is intended as a validation for the numerical method proposed before. Therefor let us continue with a discussion of source-type solutions. These are solutions of (1) with initial data $h_0(x) = c\,\delta(x)$ of the form

$$h(t,x) = t^{-\alpha} f(\eta), \qquad \eta = xt^{-\alpha}$$

where $\alpha = \frac{1}{n+4}$. It was proven by Bernis et al. (1992) that there exist no source-type solutions for $n \geq 3$, whereas for $0 < n < 3$ there exists precisely one even nonnegative source-type solution. Only for $n = 1$ an explicit expression for a source-type solution is known

$$\hat f(\eta) = \begin{cases} \frac{1}{120}(a^2 - \eta^2)^2 & \text{for } -a < \eta < a \\ 0 & \text{otherwise,} \end{cases}$$

and it was found by Smyth and Hill (1988). We use this particularly smooth solution as a first test. The general behavior of the singularity for $\eta \to a$ depends on the exponent $n$. Bernis et al. (1992) furthermore prove the asymptotics of the solution is

$$f(\eta) \sim B_1(a-\eta)^2 \qquad 0 < n < 3/2,$$
$$f(\eta) \sim B_2(a-\eta)^2(-\log(a-\eta))^{2/3} \qquad n = 3/2,$$
$$f(\eta) \sim B_3(a-\eta)^{3/n} \qquad 3/2 < n < 3$$

as $\eta \nearrow a$. The case $3/2 < n < 3$ has been further sharpened by Giacomelli et al. (2013), who proved that higher order corrections of $f$ can be written as an analytic function in two variables. In particular the next order of the expansion of $f$ is of the form

$$f(\eta) \sim B_4(a-\eta)^\nu\big(1 - b(a-\eta)^\beta + \mathcal{O}(a-\eta)^{\min\{1,2\beta\}}\big)$$

where $\nu = 3/n$ and $\beta = \frac{\sqrt{-3\nu^2+12\nu-8}-3\nu+4}{2}$. Such singularities are no particularity of source-type solutions but probably present in any moving contact line for $3/2 < n < 3$. In the case $n = 3$ contact lines do not move due to the well known contact line singularity. First we compare with the exact solution for $n = 1$. Using $h_0(x) = \hat f(x)$ with $a = 1/2$ gives the numerical and exact solution shown in fig. 3. In the finite element method we have used standard

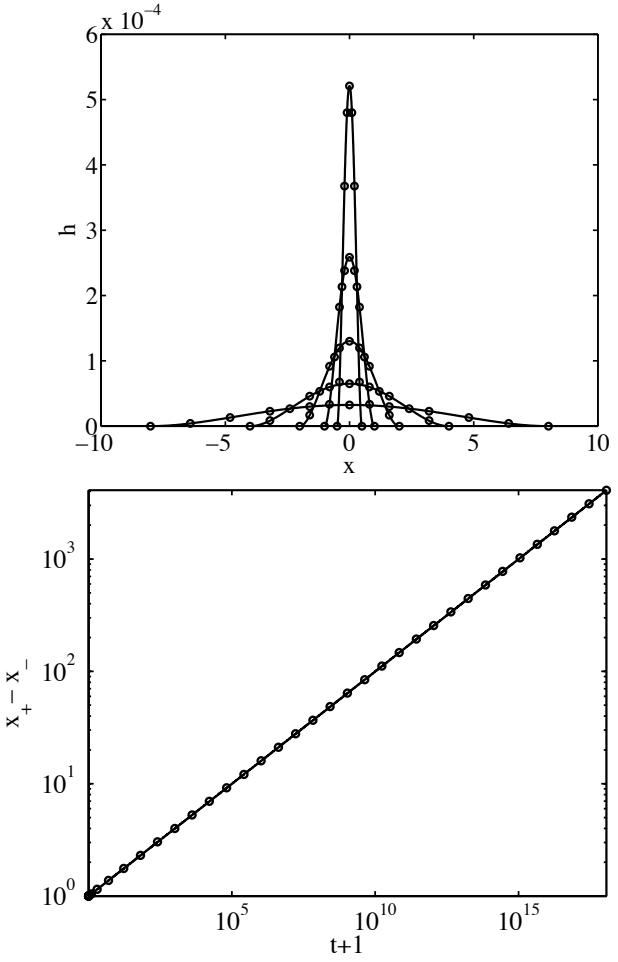


Fig. 3. Solution for $n = 1$: (upper) numerical solution with full line versus exact solution with circles at $t = 0, 2^5, 2^{10}, 2^{15}, 2^{20}$ (lower) size of the support $x_+ - x_-$ as another indicator for self-similar behavior.

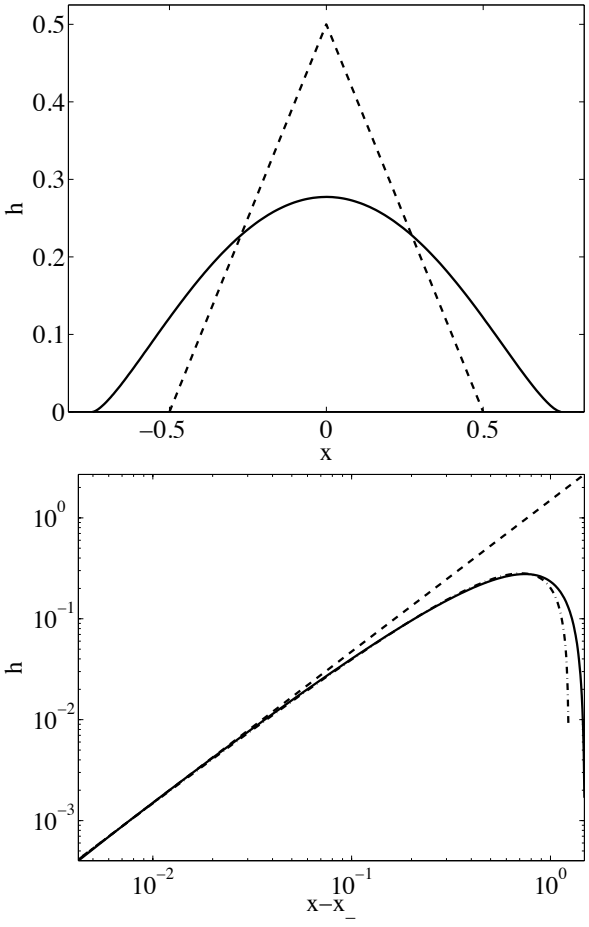


Fig. 4. (upper) initial data at $t = 0$ using dashed line and numerical solution $t = 0.1$ with full lines, (lower) singularity near $x_-$ compared to predicted $(x-x_-)^{3/2}$ behavior with dashed line and the next order correction using a dash-dotted line

linear elements with 200 elements of uniform size and a nonuniform time-step size to adjust for the slow $t^{1/5}$ dynamics of the source-type solution. To quantify the error we compare the width of the support of the numerical solution $x_+ - x_-$ with the theoretical $t^{1/5}$. As can be seen in fig. 2 even for the coarse spatial discretization the error never exceeds 1% for $t < 10^{20}$.

Let us now consider the case $n = 2$. The theoretical results for $3/2 < n < 3$ indicate that a singularity of the form$f(\eta) \sim B(a-\eta)^{3/n}$ is generic for any type of moving contact line with zero contact angle. With initial data $h_0(x) = 1/2 - |x|$ and $x_\pm = \pm 1/2$ we study to which extent this singularity can be resolved using the numerical method at a rather early time. In order to achieve this goal we use a nonuniform spatial decomposition, where the initial vertices of the finite element decomposition are at $x_i = -1/2 + (i/N)^{3/2}$ for $i = 0...N$ at $t = 0$. This allows us to resolve the later singularity near $x_-$.

Where the upper panel of fig. 4 shows that even non-smooth initial data is possible, the lower panel shows that the expected singular behavior is clearly captured in the case $n = 2$. The full line shows the computed numerical solution, whereas the dashed line shows the expected $h \sim B(a-x)^{3/2}$ behavior as $x \searrow a$ for the lowest order expansion. We further compare with the next order correction by Giacomelli et al. (2013) shown in the dash-dotted line. Similarly as for $n = 1$ now fig. 5 further underlines the convergence to a self-similar solution for $n = 2$ with $\alpha = 1/6$.

## 3. EXTENSION TO HIGHER DIMENSION

The natural extension of (1a) to higher dimensions is

$$\dot{h} + \nabla \cdot (|h|^n \nabla \Delta h) = 0,$$
$$h(0, \mathbf{x}) = h_0(\mathbf{x}),$$

on $\omega = \mathrm{supp}(h)$ with boundary conditions $|\nabla h| = 0$ on $\partial\omega$. The corresponding kinematic condition for the velocity of the boundary is

$$\dot{\mathbf{x}}(s) = \lim_{x \to s \in \partial\omega} \left( |h|^{n-1} \nabla \Delta h \right).$$

In the similar spatially discrete finite element formulation we seek $\dot{h}, \pi$ for which

$$\int_\omega (\, \dot{h}\phi + |h|^n \nabla\pi \cdot \nabla\phi) \, \mathrm{d}\omega = 0,$$
$$\int_\omega (\, \pi\varphi - \tau \nabla\dot{h} \cdot \nabla\varphi) \, \mathrm{d}\omega = \int_\omega \nabla h \cdot \nabla\varphi \, \mathrm{d}\omega,$$

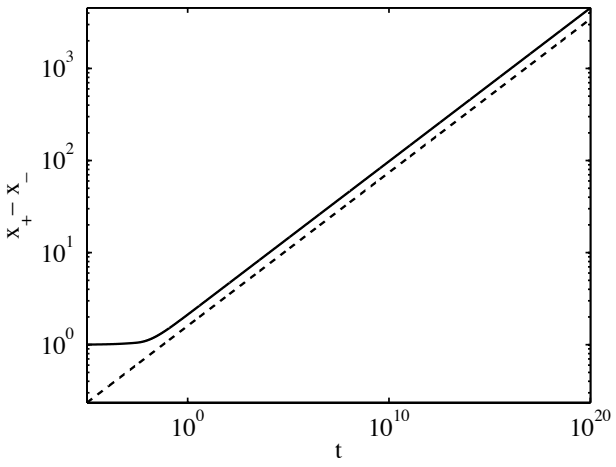


Fig. 5. size of the support $x_+ - x_-$ from numerical solution with full lines compared to theoretical $t^{1/6}$ with dashed lines as an indictor for self-similar behavior

for all test functions $\phi, \varphi$. For example in two dimension we decompose $\omega$ into pairwise disjoint triangles and define the test functions to be piecewise linear on each triangle.

The main difference to the one-dimensional case is that with the knowledge of $\dot{\mathbf{x}}$ we will still not be able to construct a map $\psi$ explicitly as in (4). Let $\mathbf{x}(t) \in \partial\omega(t)$. What we can still do is to differentiate the expression $h(t, \mathbf{x}(t)) = 0$ with respect to $t$ and obtain

$$\dot{h} + \dot{\mathbf{x}} \cdot \nabla h = 0,$$

which allows us to determine the normal component of $\dot{\mathbf{x}}$. Note that in general the choice of the tangential velocity is irrelevant when it comes to the shape of the deformed domain. Therefore we can for instance just assume $\dot{\mathbf{x}}$ to be normal to the boundary. This defines the boundary values of $\dot{\psi}$ and we can choose any extension of $\dot{\psi}$ to the inside. Later we need to take care that we use this extension to define the convectional derivative

$$\dot{H} = \dot{h} + \dot{\psi} \cdot \nabla h,$$

inside of $\omega$. One simple choice would be to let $\dot{\psi}$ satisfy $-\Delta\dot{\psi} = 0$ inside $\omega$ with the given boundary values. However, it will be very difficult to find a generic extension which is a valid deformation of the domain for all times. Unlike in one dimension it is unclear if the successive deformations of the domain will maintain an admissible decomposition of $\omega$. Here a suitable choice of the extension and also of the tangential component of $\dot{\psi}$ might be helpful.

## CONCLUSION

The algorithm that was introduced can be used to compute the evolution of solutions to the thin-film equations with compact support with zero and also with nonzero contact angle. It avoids dealing with singular higher order derivatives when evaluating the kinematic conditions and can be naturally extended to higher space dimensions. The question of a higher order method is a very interesting route to go and would probably require to resolve the singularity near the contact line much better.

## ACKNOWLEDGEMENT

I am thankful for many fruitful discussion with Robert Huth and for the financial support by DFG in the MATHEON project C10 and by Einstein Center for Mathematics in Berlin ECMath in project OT1.

## REFERENCES

Bernis, F., Peletier, L., and Williams, S. (1992). Source type solutions of a fourth order nonlinear degenerate parabolic equation. *Nonlinear Analysis: Theory, Methods & Applications*, 18(3), 217–234.

Bernis, F. and Friedman, A. (1990). Higher order nonlinear degenerate parabolic equations. *Journal of Differential Equations*, 83(1), 179–206.

Eggers, J. (2004). Toward a description of contact line motion at higher capillary numbers. *Physics of Fluids (1994-present)*, 16(9), 3491–3494.

Giacomelli, L., Gnann, M.V., and Otto, F. (2013). Regularity of source-type solutions to the thin-film equation with zero contact angle and mobility exponent between 3/2 and 3. *European Journal of Applied Mathematics*, 24(05), 735–760.

Giacomelli, L. and Knüpfer, H. (2010). A free boundary problem of fourth order: classical solutions in weighted Hölder spaces. *Communications in Partial Differential Equations*, 35(11), 2059–2091.

Grün, G. and Rumpf, M. (2000). Nonnegativity preserving convergent schemes for the thin film equation. *Numerische Mathematik*, 87(1), 113–152.

Hulshof, J., Shishkov, A.E., et al. (1998). The thin film equation with $2 \leq n < 3$: finite speed of propagation in terms of the $L^1$-norm. *Advances in Differential Equations*, 3(5), 625–642.

Smyth, N. and Hill, J. (1988). High-Order Nonlinear Diffusion. *IMA Journal of Applied Mathematics*, 40(2), 73–86.

Zhornitskaya, L. and Bertozzi, A.L. (1999). Positivity-preserving numerical schemes for lubrication-type equations. *SIAM Journal on Numerical Analysis*, 37(2), 523–555.